Engineering Science and Technology, an International Journal ■■ (2015) ■■–■■

HOSTED BY

ELSEVIER

Contents lists available at ScienceDirect

Engineering Science and Technology, an International Journal

journal homepage: http://www.elsevier.com/locate/jestch

Full Length Article

Heat and mass transfer in magnetohydrodynamic Casson fluid over an exponentially permeable stretching surface

C.S.K. Raju [a], N. Sandeep [b,*], V. Sugunamma [c], M. Jayachandra Babu [a], J.V. Ramana Reddy [c]

[a] Fluid Dynamics Division, VIT University, Vellore 632014, India
[b] Department of Mathematics, Gulbarga University, Gulbarga 585106, India
[c] Department of Mathematics, Sri Venkateswara University, Tirupati 517502, India

ARTICLE INFO

Article history:
Received 30 March 2015
Received in revised form
30 April 2015
Accepted 30 May 2015
Available online

Keywords:
MHD
Casson fluid
Newtonian fluid
Radiation
Heat source
Chemical reaction
Dissipation

ABSTRACT

In this study we analyzed the flow, heat and mass transfer behavior of Casson fluid past an exponentially permeable stretching surface in presence of thermal radiation, magneticfield, viscous dissipation, heat source and chemical reaction. We presented dual solutions by comparing the results of the Casson fluid with the Newtonian fluid. The governing partial nonlinear differential equations of the flow, heat and mass transfer are transformed into ordinary differential equations by using similarity transformation and solved numerically by using Matlab bvp4c package. The effects of various non-dimensional governing parameters on velocity, temperature and concentration profiles are discussed and presented graphically. Also, the friction factor, Nusselt and Sherwood numbers are analyzed and presented in tabular form for both Casson and Newtonian fluids separately. Under some special conditions the results of the present study have an excellent agreement with existing studies for both Casson and Newtonian fluid cases.

1. Introduction

The study of non-Newtonian fluids has a variety of applications in engineering and industry especially in extraction of crude oil from petroleum products. Casson fluid is a non-Newtonian fluid which exhibits yield stress. Human blood can also be treated as a Casson fluid due to the blood cells' chain structure and the substances contained like protein, fibrinogen, rouleaux etc. Hence the Casson fluid has its own importance in scientific as well as in engineering areas. The revolution of the boundary layer behavior of a continuous stretching surface started with Sikiadis [1]. Heat transfer characteristics of Casson fluid flow through an exponentially stretching sheet in presence of porous medium and thermal radiation was discussed by Pramanik [2] and concluded that an increase in the value of Casson parameter suppresses the velocity field. Gnaneswara Reddy [3] investigated an unsteady two-dimensional flow of a non-Newtonian fluid past a stretching surface in presence of thermal radiation and variable thermal conductivity. Khalid et al. [4] studied the unsteady free convection flow of Casson fluid past an oscillating vertical plate with constant wall temperature. Three-dimensional MHD boundary layer flow of Casson nanofluid through a linearly stretching surface with convective boundary condition was depicted by Nadeem et al. [5]. Akbar [6] studied the exact solutions of the magneticfield effect on peristaltic flow of a Casson fluid in an asymmetric channel in presence of crude oil refinement. MHD flow of Casson fluid over a stretching surface in presence of Dufour and Soret effects was analyzed by Hayat et al. [7]. Khalid et al. [8] discussed an unsteady free convection MHD flow of Casson fluid through an oscillating vertical plate embedded in a porous medium with constant wall temperature. The stagnation-point flow of non-Newtonian incompressible Casson fluid past a stretching surface in presence of Dufour and Soret effects was depicted by Kameswarani et al. [9], in this study they showed that shrinking case reduces the velocity boundary layer thickness and enhances the concentration boundary layer thickness. Hussanan et al. [10] investigated the heat transfer and Newtonian fluid analysis on an unsteady boundary layer flow of a Casson fluid through an oscillating vertical plate.

An unsteady two-dimensional Casson fluid flow of non-Newtonian fluid past a stretching surface in presence of porous medium was illustrated by Kirubhashankar et al. [11]. A three-dimensional MHD Casson fluid flow over a linearly stretching surface in porous medium was examined by Nadeem et al. [12] and concluded that the increase in magneticfield, Casson parameter decreases the velocity profiles in both x and y directions. Haq et al. [13] investigated the suction/injection effects on magnetohydrodynamic flow of a Casson

* Corresponding author. Tel.: +918220636617; fax: +918220636617.
E-mail address: nsreddy.dr@gmail.com (N. Sandeep).
Peer review under responsibility of Karabuk University.

http://dx.doi.org/10.1016/j.jestch.2015.05.010

Please cite this article in press as: C.S.K. Raju, N. Sandeep, V. Sugunamma, M. Jayachandra Babu, J.V. Ramana Reddy, Heat and mass transfer in magnetohydrodynamic Casson fluid over an exponentially permeable stretching surface, Engineering Science and Technology, an International Journal (2015), doi: 10.1016/j.jestch.2015.05.010

nanofluid past a permeable exponentially shrinking surface and concluded that non-Newtonian fluid have higher friction factor compared with Newtonian fluid. Boundary layer analysis of Casson fluid flow past an exponentially permeable shrinking surface in presence of magneticfield was examined analytically by Nadeem et al. [14]. Recently Malik et al. [15] discussed the heat transfer and boundary layer flow of Casson nanofluid flow past a vertical exponentially stretching cylinder. Stagnation point flow of optimized analytical solution for oblique flow of Casson-nanofluid with convective boundary conditions was illustrated by Nadeem et al. [16]. Carmona et al. [17] presented the transpose diffusive term for viscoelastic type non-Newtonian fluid flow using numerical analysis of variable collocated arrangement. Reynolds number impact on the flow of electro rheological fluid of a Casson type between fixed sheets of revolution was discussed by Walicka and Falicki [18]. Animasaun et al. [19] studied an incompressible laminar free convective MHD Casson fluid flow past an exponentially stretching sheet with suction by using homotopy analysis method. They concluded that increasing values of variable plastic dynamic viscosity parameter of Casson fluid correspond to enhanced velocity profiles and reduce the temperature throughout the boundary layer. The effect of magneticfield and heat source on the steady boundary layer flow and heat transfer of a Casson nanofluid past a vertical exponentially stretching cylinder across its radial direction was discussed by Sarojamma and Vendabai [20].

Immanuel et al. [21] analyzed the viscous steady flow of Casson fluid with fixed velocity under the influence of uniform magneticfield. A two-dimensional non-linear squeezing flow of Casson fluid between horizontal plates was investigated analytically by Ganesh et al. [22]. Wahiduzzaman et al. [23] illustrated an unsteady incompressible MHD non-Newtonian Casson fluid flow of an electrically conducting fluid between parallel porous plates with Hall Effect. Magneto hydrodynamics Casson fluid flow through a non-isothermal linearly stretching surface in presence of porous medium was depicted by Wahiduzzaman et al. [24]. Singh and Dandapat [25] studied the transverse uniform magneticfield effect on thin film flow of Casson liquid past a nonlinearly stretching surface. Rees and Bassom [26] examined an unsteady free convection thermal boundary layer flow of Bingham fluid in a saturated porous medium. An unsteady free convection flow of a viscous dusty fluid between two flat plates filled with porous medium in presence of inclined magneticfield was considered by Sandeep and Sugunamma [27]. Sandeep et al. [28] discussed an unsteady natural convective flow of nanofluid past an infinite vertical plate in presence of radiation effect. Mohan Krishna et al. [29] elaborated this work by choosing heat source effect and various nanofluids. MHD convection nanofluid flow past a moving vertical plate in presence of Soret and radiation effects was discussed by Raju et al. [30]. MHD boundary layer flow due to an exponentially stretching sheet in presence of radiation was discussed by Ishak [31]. Analytical solution for third grade nanofluid flow over a rotating vertical cone was presented by Nadeem and Saleem [32]. Nadeem et al. [33] analyzed MHD oblique flow of Walter's B type fluid over a convective surface. Nadeem and Saleem [34] investigated an optimized study of mixed convection flow of a Jeffrey nanofluid on a Rotating Vertical Cone. A combined effect of magnetic field and partial slip on obliquely striking rheological fluid over a stretching surface was discussed by Nadeem et al. [35].

Present study is the extension work of Pramanik [2]. In this study we analyzed the flow, heat and mass transfer behavior of Casson fluid past an exponentially permeable stretching surface in presence of thermal radiation, uniform magneticfield, viscous dissipation, heat source and chemical reaction. We presented dual solutions by comparing the results of the Casson fluid with the Newtonian fluid. The governing partial nonlinear differential equations of the flow, heat and mass transfer are transformed into ordinary differential equations by using similarity transformation and solved numerically. The effects of various non-dimensional governing parameters on velocity, temperature and concentration profiles are discussed and presented graphically. Also, the friction factor and Nusselt and Sherwood numbers are analyzed and given in tabular form for both Casson and Newtonian fluids separately. Under some special conditions the results of the present study have an excellent agreement with existing studies.

2. Mathematical formulation

Consider a steady, incompressible, dissipative MHD Casson fluid past a nonlinearly exponentially stretching sheet which coincides with the plane $y=0$. The fluid flow is confined to $y>0$. We applied a variable magneticfield and there is no applied voltage, which implies the absence of an electric field. Also it is assumed that the induced magnetic field is small compared to the external magnetic field. This implies that a small magnetic Reynolds number exists in this study. Along with this we considered heat source and chemical reaction to the flow. Two equal and opposite forces are applied along the x axis, so that the wall is stretched keeping the origin fixed. The rheological equation of state for an isotropic and incompressible flow of a Casson fluid is as follows:

$$\tau_{ij}=\begin{cases}2\left(\mu_B+p_y/\sqrt{2\pi}\right)e_{ij}, & \pi>\pi_c\\ 2\left(\mu_B+p_y/\sqrt{2\pi}\right)e_{ij} & \pi<\pi_c\end{cases}.$$

here $\pi=e_{ij}e_{ij}$ and e_{ij} are the $(i,j)^{th}$ component of the deformation rate, π is the product of the component of the deformation rate with itself, π_c is a critical value of this product based on the non-Newtonian model, μ_B is plastic dynamic viscosity of non-Newtonian fluid, and p_y is the yield stress of the fluid. The equations governing the flow can be written as

$$\frac{\partial u}{\partial x}+\frac{\partial u}{\partial y}=0, \tag{1}$$

$$u\frac{\partial u}{\partial x}+v\frac{\partial u}{\partial y}=v\left(1+\frac{1}{\beta}\right)\frac{\partial^2 u}{\partial y^2}+g\beta_T(T-T_\infty)+g\beta_c(C-C_\infty)-\frac{\sigma B^2 u}{\rho}, \tag{2}$$

$$u\frac{\partial T}{\partial x}+v\frac{\partial T}{\partial y}=\frac{k}{\rho c_p}\frac{\partial^2 T}{\partial y^2}-\frac{1}{\rho c_p}\frac{\partial q_r}{\partial y}+\frac{\mu}{\rho c_p}\left(1+\frac{1}{\beta}\right)\left(\frac{\partial u}{\partial y}\right)^2-\frac{Q}{\rho c_p}(T-T_\infty), \tag{3}$$

$$u\frac{\partial C}{\partial x}+v\frac{\partial C}{\partial y}=D_m\frac{\partial^2 C}{\partial y^2}-k_l(C-C_\infty), \tag{4}$$

With the boundary conditions

$$\begin{aligned}&u=U,\quad v=-V(x),\quad T=T_w,\quad C=C_w \quad \text{at}\quad y=0,\\ &u\to 0,\quad T\to T_\infty,\quad C\to C_\infty \quad\qquad\quad \text{as}\quad y\to\infty,\end{aligned} \tag{5}$$

where u and v are the velocity components in the x,y directions, ν is the kinematic viscosity, ρ is the fluid density, $\beta=\mu_B\sqrt{2\pi_c}/p_y$ is the Casson fluid parameter, g is the acceleration due to gravity, β_T is the thermal expansion coefficient, T is the fluid temperature, β_c is the concentration expansion coefficient, σ is electric conductivity, $B=B_0e^{Nx/2L}$ is the variable magneticfield, k is the thermal conductivity of the fluid, ρc_p is the heat capacitance of fluid, q_r is the radiative heat flux, μ is the dynamic viscosity, $Q=Q_0e^{Nx/L}$ is the variable heat source parameter, D_m is the coefficient of the mass diffusivity, C is the concentration of the fluid, $k_l=k_0e^{Nx/L}$ is the chemical reaction parameter, N is the exponential parameter and $V(x)=v_0e^{Nx/2L}$ is the suction/injection parameter.

The radiative heat flux q_r under Rosseland approximation (Brewster [36]) has the form

Please cite this article in press as: C.S.K. Raju, N. Sandeep, V. Sugunamma, M. Jayachandra Babu, J.V. Ramana Reddy, Heat and mass transfer in magnetohydrodynamic Casson fluid over an exponentially permeable stretching surface, Engineering Science and Technology, an International Journal (2015), doi: 10.1016/j.jestch.2015.05.010

$$q_r = -\frac{4\sigma^*}{3k^*}\frac{\partial T^4}{\partial y}, \tag{6}$$

where σ^* is the Stefan–Boltzmann constant and k^* is the mean absorption coefficient. The temperature differences within the flow are assumed to be sufficiently small such that T^4 may be expressed as a linear function of temperature. Expanding T^4 using Taylor series and neglecting higher order terms yields $T^4 \cong 4T_\infty^{\,3}T - 3T_\infty^{\,4}$, then equation (3) becomes

$$\left(u\frac{\partial T}{\partial x} + v\frac{\partial T}{\partial y}\right) = \frac{k}{\rho c_p}\frac{\partial^2 T}{\partial y^2} - \frac{1}{\rho c_p}\frac{16\sigma T_\infty^{\,3}}{3\rho c_p k^*}\frac{\partial^2 T}{\partial y^2} + \frac{\mu}{\rho c_p}\left(1+\frac{1}{\beta}\right)\left(\frac{\partial u}{\partial y}\right)^2 - Q(T-T_\infty) \tag{7}$$

We now employ the similarity transformation as

$$\eta = \sqrt{U_0/2\nu L}e^{Nx/2L}y, \quad v = -\sqrt{\frac{\nu U_0}{2L}}e^{Nx/2L}N\{f(\eta)+\eta f'(\eta)\},$$
$$u = U_0 e^{Nx/L}f'(\eta), \quad T = T_\infty + T_0 e^{2Nx/L}, \quad C = C_\infty + C_0 e^{2Nx/L}, \tag{8}$$

where T_∞ is the ambient fluid temperature, C_∞ is the ambient fluid concentration, L is the characteristic length, U_0 is the fluid velocity.

Using equations (5), (7) and (8), equations (2)–(4) transformed to the ordinary differential equations is of the form

$$\left(1+\frac{1}{\beta}\right)f''' + N(ff'' - 2f'^2) + 2Gr\theta + 2Gc\phi - Mf' = 0 \tag{9}$$

$$\frac{1}{\Pr}\left(\frac{4}{3}R_a + 1\right)\theta'' + N(4f'\theta - f\theta') + \left(1+\frac{1}{\beta}\right)Ecf''^2 - Q_H\theta = 0 \tag{10}$$

$$\phi'' + NSc(4f'\phi - f\phi') - ScK_l\phi = 0 \tag{11}$$

The transformed boundary conditions are

$$f(\eta) = S, \quad f'(\eta) = 1, \quad \theta(\eta) = 1, \quad \phi(\eta) = 1 \quad \text{at} \quad \eta = 0, \tag{12}$$

$$f'(\eta) \to 0, \quad \theta(\eta) \to 0, \quad \phi(\eta) \to 0 \quad \text{as} \quad \eta \to \infty, \quad \text{as}$$

where primes denote differentiation with respect to η, $S = \frac{v_0}{\sqrt{U_0\nu/2L}}$, S is the suction for $S>0$ and $S<0$ for injection, β is the Casson fluid parameter, $M = \sigma B_0^{\,2}/\rho u_0$ is the magneticfield parameter, N is the exponential parameter, $Gr = g\beta LT_0/U_0^{\,2}$ is thermal Grashof number, $Gc = G\beta LC_0/U_0^{\,2}$ is the concentration Grashof number, $\Pr = \upsilon_f/\alpha_f$ is the Prandtl number, $R_a = 4\sigma^* T_\infty^3/k^* k$ is the radiation parameter, $Ec = U_0^{\,2}/Lc_p$ is the Eckert number, $Q_H = Q_0 L/T_0 U_0$ is the heat source parameter, $Sc = \upsilon_f/D_m$ is the Schmidt number, $K_l = k_0 L/C_0 U_0$ is the chemical reaction parameter.

The physical quantities of interest are the local skin friction coefficient, the wall heat transfer coefficient and mass transfer coefficients are given by

$$Cf_x \,\mathrm{Re}_x^{1/2} = f''(0), \tag{13}$$

$$Nu_x \,\mathrm{Re}_x^{-1/2} = -\theta'(0), \tag{14}$$

$$Sh_x \,\mathrm{Re}_x^{-1/2} = -\phi'(0), \tag{15}$$

3. Results and discussion

The system of nonlinear ordinary differential equations (9) to (11) with the boundary conditions (12) are solved numerically by using bvp4c with MATLAB package. The obtained results show the effects of the various non-dimensional governing parameters, namely exponential parameter (N), magneticfield parameter (M), radiation parameter (R_a), Eckert number (Ec), heat source parameter (Q_H) and chemical reaction parameter (K_l) on the flow, temperature and concentration profiles. Also, the friction factor and Nusselt and Sherwood numbers are discussed and given in tabular form. For numerical results we used $Ec = 0.1$, $M = 1, Gr = Gc = 1, S = 0.5, \Pr = 0.7$, $Sc = 0.6, N = 1, R_a = Q_H = K_l = 0.5$. These values are treated as common throughout the study except the varied values in respective figures and tables.

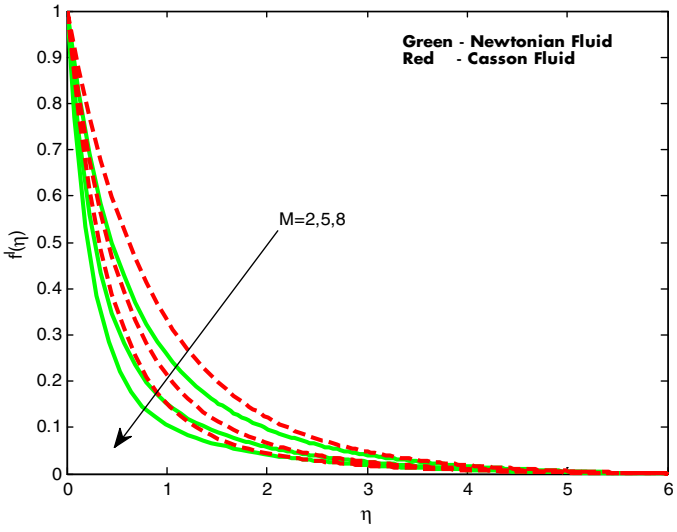

Fig. 1. Velocity profiles for different values of magneticfield parameter M.

Figures 1–3 depict the effect of magneticfield parameter on velocity, temperature and concentration profiles respectively. It is clear from the figures that an increase in the magneticfield parameter enhances the temperature and concentration boundary layers and reduces the velocity boundary layer. This is due to the fact that an increase in magneticfield develops the opposite force to the flow direction, which is called Lorentz force. This force we have has the tendency to reduce the velocity boundary layer and enhance the thermal boundary layer thickness. It is also interesting to mention

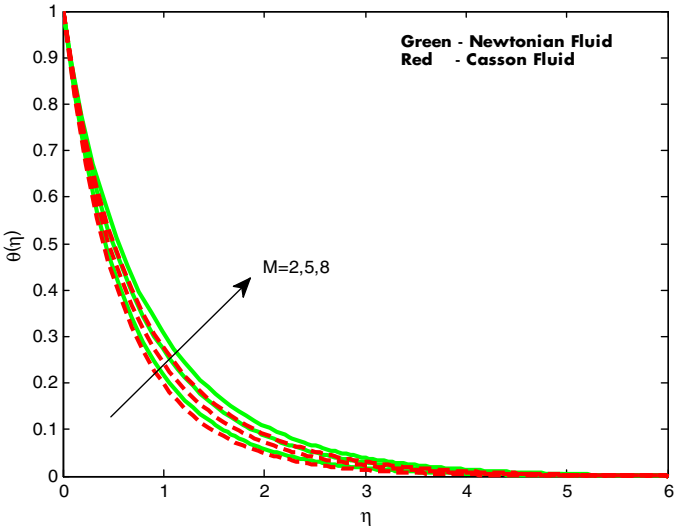

Fig. 2. Temperature profiles for different values of magneticfield parameter M.

Please cite this article in press as: C.S.K. Raju, N. Sandeep, V. Sugunamma, M. Jayachandra Babu, J.V. Ramana Reddy, Heat and mass transfer in magnetohydrodynamic Casson fluid over an exponentially permeable stretching surface, Engineering Science and Technology, an International Journal (2015), doi: 10.1016/j.jestch.2015.05.010

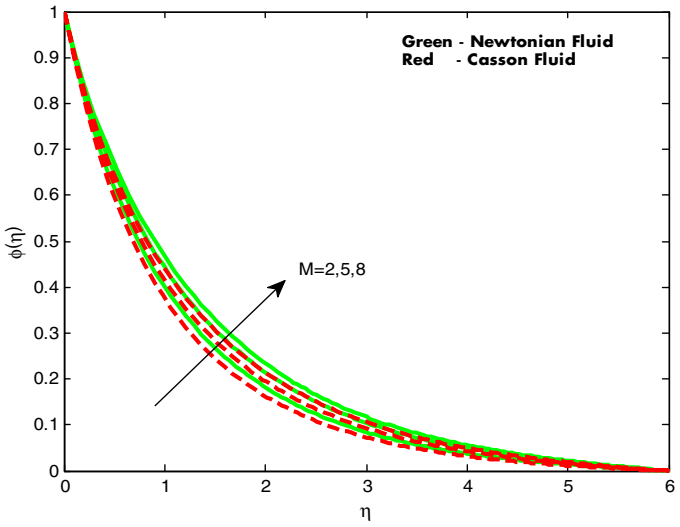

Fig. 3. Concentration profiles for different values of magneticfield parameter M.

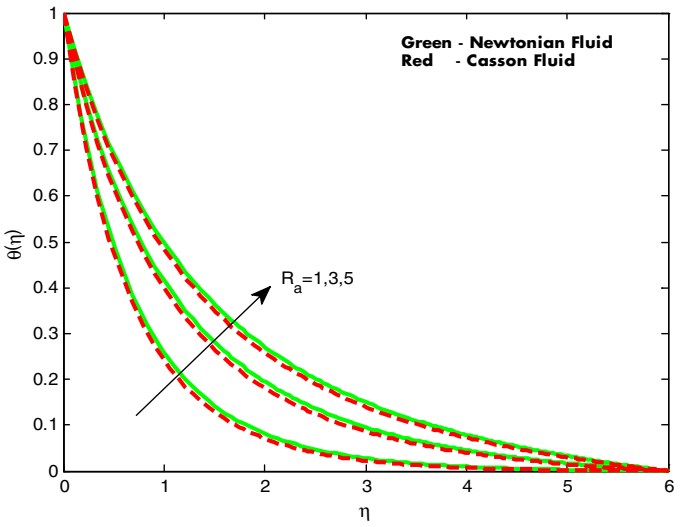

Fig. 5. Temperature profiles for different values of radiation parameter R_a.

that the temperature profiles of the Casson fluid effectively enhances compared with the temperature profiles of Newtonian fluid.

The influence of radiation parameter (R_a) on velocity and temperature profiles is shown in Figs. 4 and 5. It can be observed that there is an enhancement in the velocity and temperature profiles when there is an increase in the radiation parameter. This may happen due to the fact that an increase in the radiation parameter enhances the thermal boundary layer. In view of this we can conclude that influence of radiation is more significant as $R_a \to 0\,(R_a \neq 0)$ and it can be neglected as $R_a \to \infty$. This agrees with the general physical behavior of the radiation parameter. Also, it is observed that an increase in radiation parameter shows more impact on the velocity and temperature profiles of the Casson fluid compared with the Newtonian fluid.

Figures 6–8 depict the influence of the exponential parameter on velocity, temperature and concentration profiles. It is evident from the figures that an increase in exponential parameter declines the velocity, temperature and concentration boundary layers. This happens due to the decreasing nature of the momentum, thermal and concentration profiles with the increasing value of the exponential parameter (N). This may happen due to a decrease in the wall temperature throughout the boundary layer for positive values of exponential parameter (i.e. heat transfer takes place from the wall to ambient fluid, which causes the particles to move away from the wall).

The influence of chemical reaction parameter on velocity and concentration profiles is displayed in Figs. 9 and 10. It can be observed from the figures that a rise in the value of chemical reaction parameter (K_l) reduces the momentum and concentration boundary layers. Due to an increase in the interfacial mass transfer we observed a fall in velocity and concentration profiles. This enhancement in the interfacial mass transfer causes the improvement of the Sherwood number.

Figure 11 displays the effect of heat source parameter on temperature profiles of the flow. It is noticed that an increase in the heat source parameter (Q_H) reduces the temperature profiles of the flow. It is expected that an increase in heat source parameter will release the heat energy to the flow, which causes the temperature

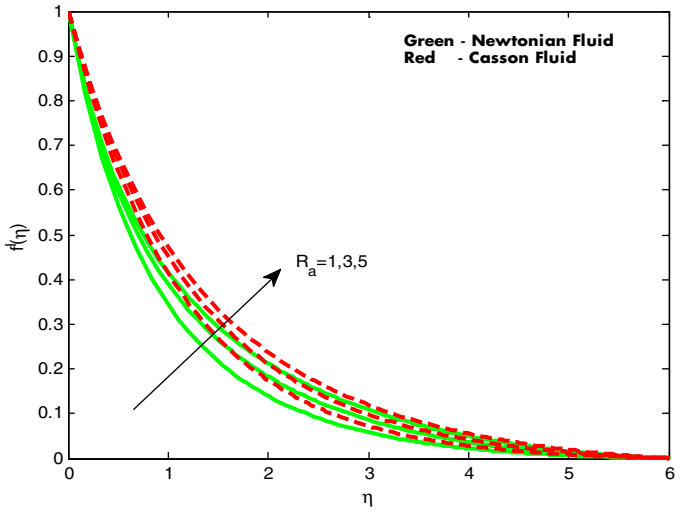

Fig. 4. Velocity profiles for different values of radiation parameter R_a.

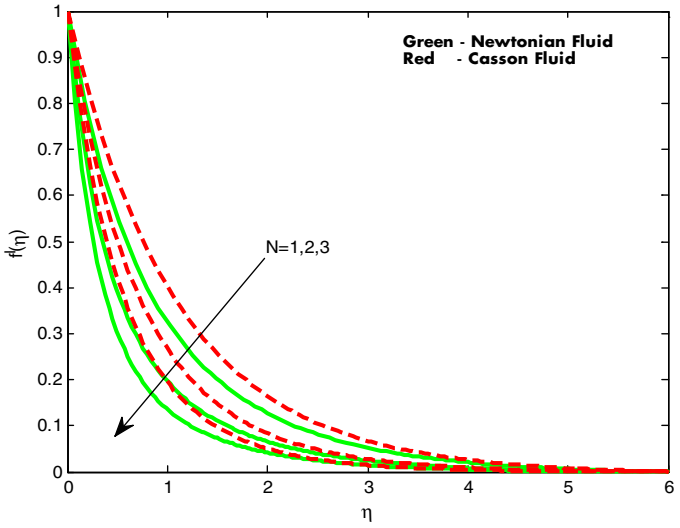

Fig. 6. Velocity profiles for different values of exponential parameter N.

Please cite this article in press as: C.S.K. Raju, N. Sandeep, V. Sugunamma, M. Jayachandra Babu, J.V. Ramana Reddy, Heat and mass transfer in magnetohydrodynamic Casson fluid over an exponentially permeable stretching surface, Engineering Science and Technology, an International Journal (2015), doi: 10.1016/j.jestch.2015.05.010

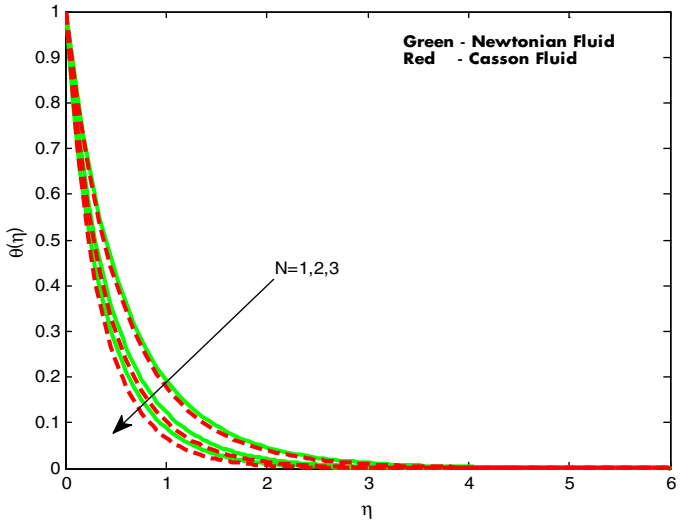

Fig. 7. Temperature profiles for different values of exponential parameter N.

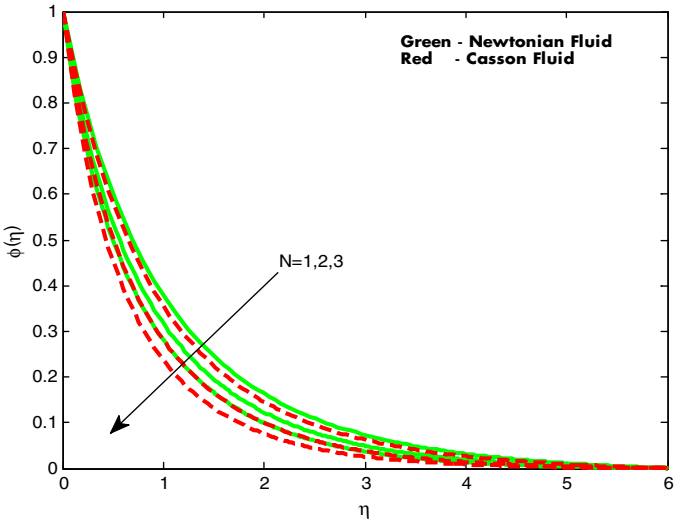

Fig. 8. Concentration profiles for different values of exponential parameter N.

profiles to enhance. But due to the domination of the external heat compared with the heat source supplied to the flow, we noticed reverse results to that of expected results. The influence of viscous dissipation parameter (Ec) on velocity and the temperature profiles are shown in Figs. 12 and 13. It is observed from the figures that an increase in the Eckert number enhances the flow and thermal boundary layer thickness. This is due to the fact that an increase in dissipation improves the thermal conductivity of the flow. This helps to enhance the thermal and momentum boundary layers.

Table 1 shows the comparison of the present results for Newtonian fluid case with the existing results of Pramanik [2] and Ishak [31] and Table 2 shows the comparison of the present results with the existing results of Pramanik [2] for the dimensionless thermal boundary layer thickness of Casson fluid $\eta_{\delta_h} = (v/U_0)^{-1/2}\delta_h$, where δ_h is the thermal boundary layer thickness. Present results have an excellent agreement with the existing studies for both Newtonian and Casson fluid cases. This shows the validity of the present results along with the accuracy of the numerical method we used in this study. Tables 3 and 4 represent the influence of the non-dimensional governing parameters on Skin friction coefficient $f''(0)$, Nusselt number $-\theta'(0)$ and Sherwood number $-\phi'(0)$ for Newtonian and Casson fluids respectively. It is observed from the tables that an increase in the magneticfield parameter reduces the friction factor, heat and mass transfer rate. A rise in the values of radiation parameter, thermal Grashof number and Eckert number enhances the friction factor, mass transfer rate and declines the rate of heat transfer. An increase in chemical reaction parameter and Schmidt number depreciates the friction factor and Nusselt number, but enhances the mass transfer rate. Enhancement in heat source parameter and Prandtl number increases the heat transfer rate and declines the mass transfer rate along with skin friction coefficient. A rise in the thermal Grashof number increases the friction factor, heat and mass transfer rate. An increase in the value of exponential parameter depreciates the friction factor and enhances the Nusselt and Sherwood numbers for both Newtonian and Casson fluids.

Table 1
Comparison of the values of $-\theta'(0)$ for Newtonian fluid.

Pr	Pramanik [2]	Ishak [31]	Present study
1	0.9547	0.9548	0.954734
2	1.4714	1.4715	1.471426
3	1.8691	1.8691	1.869134
5	2.5001	2.5001	2.500102
10	3.6603	3.6603	3.660312

When $S = R_a = Gr = Gc = 0$, $K_l = Q_H = Sc = 0$.

Table 2
Comparison of the values of dimensionless thermal boundary layer thickness η_{δ_h} for Casson fluid.

β	Pramanik [2]			Present study		
	$S=-0.5$	$S=0$	$S=0.5$	$S=-0.5$	$S=0$	$S=0.5$
0.2	5.73	4.61	3.78	5.7321	4.6132	3.7812
0.5	7.03	5.47	4.34	7.0310	5.4723	4.3421
0.8	7.71	5.96	4.65	7.7131	5.9632	4.6523
1	7.99	6.19	4.79	7.9910	6.1903	4.7942
2	8.62	6.80	5.17	8.6210	6.8021	5.1702
5	9.00	7.30	5.50	9.0000	7.3001	5.5010

When $R_a = Gr = Gc = K_l = Q_H = Sc = 0, N = 1, \Pr = 0.7$.

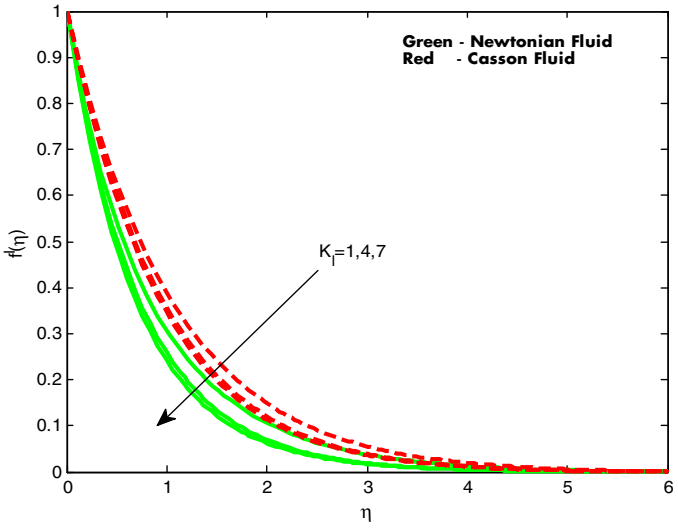

Fig. 9. Velocity profiles for different values of chemical reaction parameter K_l.

Please cite this article in press as: C.S.K. Raju, N. Sandeep, V. Sugunamma, M. Jayachandra Babu, J.V. Ramana Reddy, Heat and mass transfer in magnetohydrodynamic Casson fluid over an exponentially permeable stretching surface, Engineering Science and Technology, an International Journal (2015), doi: 10.1016/j.jestch.2015.05.010

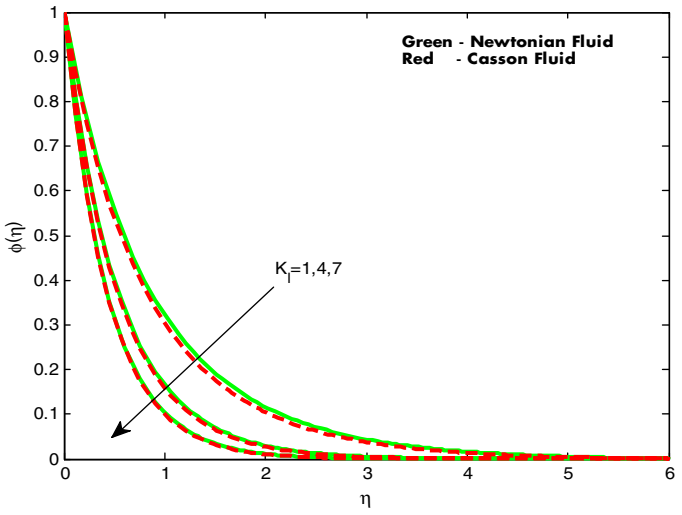

Fig. 10. Concentration profiles for different values of chemical reaction parameter K_l.

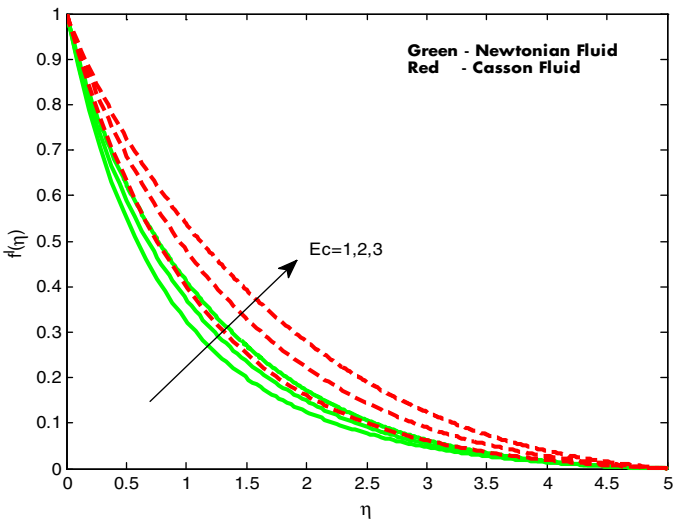

Fig. 12. Velocity profiles for different values of viscous dissipation parameter Ec.

4. Conclusions

This study presented the flow, heat and mass transfer behavior of Casson fluid past an exponentially permeable stretching surface in presence of thermal radiation, magneticfield, viscous dissipation, heat source and chemical reaction. We presented dual solutions by comparing the results of the Casson fluid with the Newtonian fluid. The governing partial nonlinear differential equations of the flow, heat and mass transfer are transformed into ordinary differential equations by using similarity transformation and solved numerically by using Matlab bvp4c package. The effects of various non-dimensional governing parameters on velocity, temperature and concentration profiles are discussed and presented graphically. Also, the friction factor and Nusselt and Sherwood numbers are analyzed and given in tabular form for both Casson and Newtonian fluids separately. The conclusions are as follows:

- An increase in exponential parameter and heat source parameter enhances the heat transfer rate.
- Magneticfield parameter and chemical reaction parameter have the tendency to reduce the skin friction coefficient.
- A rise in the values of radiation parameter, thermal and concentration Grashof numbers enhances the mass transfer rate.
- An increase in viscous dissipation parameter enhances the velocity and thermal boundary layers.
- Casson fluid showed better heat transfer performance compared with Newtonian fluid.

Acknowledgements

The authors wish to express their thanks to the very competent anonymous referees for their valuable comments and suggestions. The second author acknowledges the UGC for financial support under the UGC Dr. D. S. Kothari Fellowship Scheme (No. F.4-2/2006 (BSR)/MA/13-14/0026).

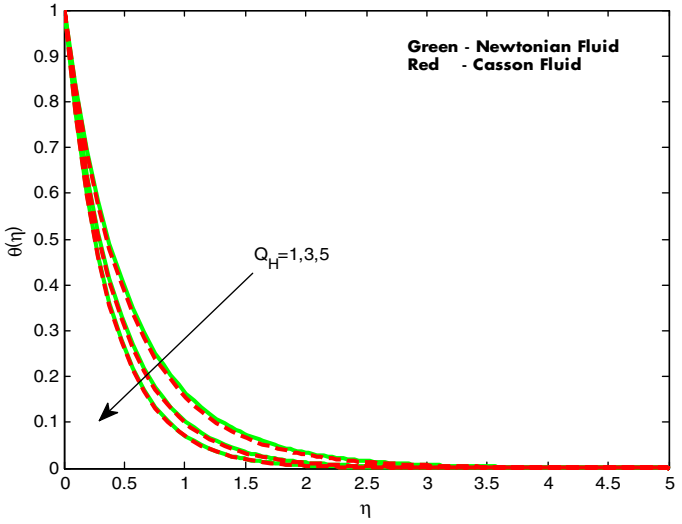

Fig. 11. Temperature profiles for different values of heat source parameter Q_H.

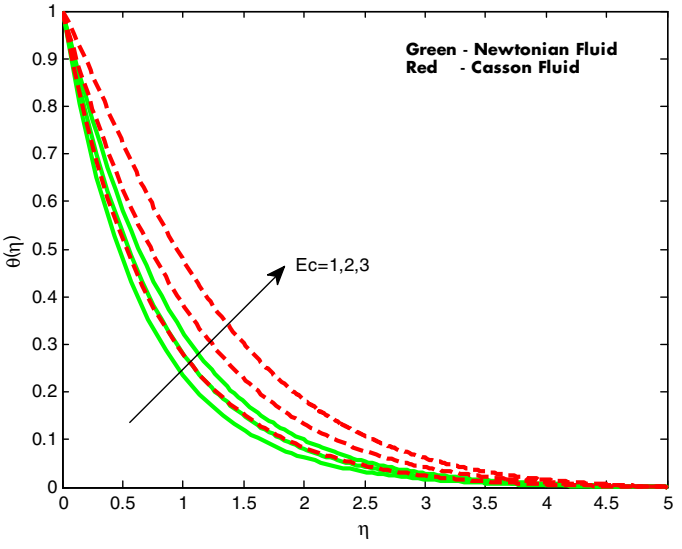

Fig. 13. Temperature profiles for different values of viscous dissipation parameter Ec.

Please cite this article in press as: C.S.K. Raju, N. Sandeep, V. Sugunamma, M. Jayachandra Babu, J.V. Ramana Reddy, Heat and mass transfer in magnetohydrodynamic Casson fluid over an exponentially permeable stretching surface, Engineering Science and Technology, an International Journal (2015), doi: 10.1016/j.jestch.2015.05.010

Table 3
Variation in $f''(0), -\theta'(0)$ and $-\phi'(0)$ for Newtonian fluid.

M	R_a	K_l	Q_H	N	Gr	Gc	Ec	Pr	Sc	$f''(0)$	$-\theta'(0)$	$-\phi'(0)$
1										1.767436	2.305390	1.351317
3										0.699768	2.201769	1.271489
5										–0.163139	2.104417	1.209886
	1									1.916400	1.918780	1.367787
	2									2.107244	1.503753	1.391441
	3									2.229523	1.274035	1.407805
		1								1.699141	2.292466	1.465677
		4								1.432580	2.243850	2.010816
		7								1.273196	2.217004	2.431079
			1							1.733597	2.403173	1.347692
			4							1.578958	2.915278	1.332762
			7							1.471243	3.344625	1.323644
				1						1.767436	2.305390	1.351317
				2						0.082506	3.129659	1.714151
				3						–1.204888	3.775832	1.993520
					1					0.421137	2.219323	1.288666
					10					3.343361	2.363161	1.416351
					20					6.287771	2.370790	1.522246
						1				0.053372	2.139444	1.229996
						10				3.697718	2.394336	1.455418
						20				7.166802	2.380120	1.601168
							0.2			1.781683	2.276165	1.353411
							0.4			1.809733	2.216713	1.357547
							0.6			1.837184	2.155875	1.361612
								0.2		2.287157	1.173732	1.415747
								0.4		2.012243	1.700651	1.379336
								0.6		1.836221	2.118882	1.358692
									0.2	2.158595	2.369666	0.758934
									0.4	1.926462	2.332591	1.089813
									0.6	1.767436	2.305390	1.351317

Table 4
Variation in $f''(0), -\theta'(0)$ and $-\phi'(0)$ for Casson fluid.

M	R_a	K_l	Q_H	N	Gr	Gc	Ec	Pr	Sc	$f''(0)$	$-\theta'(0)$	$-\phi'(0)$
1										0.632831	2.252842	1.328818
3										0.060982	2.165744	1.266976
5										–0.405310	2.081927	1.218755
	1									0.724013	1.872246	1.341146
	2									0.847243	1.465601	1.359431
	3									0.930237	1.241437	1.372512
		1								0.585278	2.241479	1.444886
		4								0.410815	2.200590	1.996156
		7								0.313552	2.178935	2.419693
			1							0.611091	2.353823	1.325925
			4							0.515959	2.879126	1.314280
			7							0.453266	3.316071	1.307420
				1						0.632831	2.252842	1.328818
				2						–0.311621	3.107235	1.729534
				3						–1.003121	3.797861	2.051347
					1					–0.029040	2.189420	1.284498
					10					1.420005	2.296287	1.376869
					20					2.915928	2.297128	1.458533
						1				–0.255231	2.124799	1.243116
						10				1.643761	2.319238	1.406246
						20				3.478032	2.283440	1.518675
							0.2			0.648469	2.227656	1.331782
							0.4			0.678291	2.178821	1.337480
							0.6			0.706205	2.131590	1.342868
								0.2		0.970475	1.143754	1.378995
								0.4		0.784964	1.658260	1.349985
								0.6		0.674426	2.069061	1.334302
									0.2	0.917129	2.311618	0.746360
									0.4	0.744912	2.277426	1.071306
									0.6	0.632831	2.252842	1.328818

Please cite this article in press as: C.S.K. Raju, N. Sandeep, V. Sugunamma, M. Jayachandra Babu, J.V. Ramana Reddy, Heat and mass transfer in magnetohydrodynamic Casson fluid over an exponentially permeable stretching surface, Engineering Science and Technology, an International Journal (2015), doi: 10.1016/j.jestch.2015.05.010

References

[1] B.C. Sikiadis, Flow past a continuously moving plate, A. I. Ch. E. J. 7 (1961) 26–32.
[2] S. Pramanik, Casson fluid flow and heat transfer past an exponentially porous stretching sheet in presence of thermal radiation, Ain Shams Eng. J. 5 (2014) 205–212.
[3] M. Gnaneswara Reddy, Unsteady radiative-convective boundary layer flow of a Casson fluid with variable thermal conductivity, J. Eng. Phys. Thermo Phys. 88 (1) (2015) 240–251.
[4] A. Khalid, I. Khan, S. Shafiel, Exact solutions for unsteady free convection flow of a Casson fluid over an oscillating vertical plate with constant wall temperature, Abstr. Appl. Anal. (15) (2015) 946350 <http://dx.doi.org/10.1155/2015/946350>.
[5] S. Nadeem, R.L. Haq, N.S. Akbar, MHD three-dimensional boundary layer flow of Casson nanofluid past a linearly stretching sheet with convective boundary conditions, IEEE Trans. Nanotechnol. 13 (1) (2014) 109–115, doi:10.1109/TNANO.2013.2293735.
[6] N. Akbar, Influence of magnetic field on peristaltic flow of a Casson fluid in an asymmetric channel: application in crude oil refinement, J. Magnet. Magnet. Mater. 378 (2015) 463–468.
[7] T. Hayat, S.A. Shehzad, A. Alsaedi, Soret and Dufour effects on magnetohydrodynamic (MHD) flow of Casson fluid, Appl. Math. Mech. 33 (10) (2012) 1301–1312.
[8] A. Khalid, I. Khan, A. Khan, S. Shafie, Unsteady MHD free convection flow of Casson fluid past over an oscillating vertical plate embedded in a porous medium, Eng. Sci. Technol. Int. J. (2015) doi:10.1016/j.jestch.2014.12.006 (in press).
[9] P.K. Kameswarani, S. Shaw, P. Sibanda, Dual solutions of Casson fluid flow over a stretching or shrinking sheet, Sadhana 39 (6) (2014) 1573–1583.
[10] A. Hussanan, M. Zuki Salleh, R.M. Tahar, I. Khan, Unsteady boundary layer flow and heat transfer of a Casson fluid past an oscillating vertical plate with Newtonian heating, PLoS ONE 9 (10) (2014) e108763, doi:10.1371/journal.pone.0108763.
[11] C.K. Kirubhashankar, S. Ganesh, A. Mohamed Ismail, Casson fluid flow and heat transfer over an unsteady porous stretching surface, Appl. Math. Sci. 9 (7) (2015) 345–351.
[12] S. Nadeem, R.L. Haq, N.S. Akbar, Z.H. Khan, MHD three-dimensional Casson fluid flow past a porous linearly stretching sheet, Alex. Eng. J. 52 (2013) 577–582.
[13] R.L. Haq, S. Nadeem, Z.H. Khan, T.G. Okedayo, Convective heat transfer and MHD effects on Casson nanofluid flow over a shrinking sheet, Cent. Eur. J. Phys. 12 (12) (2014) 862–871.
[14] S. Nadeem, R.U.I. Haq, C. Lee, MHD flow of a Casson fluid over an exponentially shrinking sheet, Sci. Iran. B 19 (6) (2012) 1550–1553.
[15] M.Y. Malik, M. Naseer, S. Nadeem, A. Rehman, The boundary layer flow of Casson nanofluid over a vertical exponentially stretching cylinder, Appl. Nanosci. 4 (2014) 869–873.
[16] S. Nadeem, R. Mehmood, N. Sher Akbar, Optimized analytical solution for oblique flow of a Casson-nanofluid with convective boundary conditions, Int. J. Thermal Sci. 78 (2014) 90–100.
[17] A. Carmona, O. Lehmkuhl, C.D. Perez-Segarra, A. Oliva, Numerical analysis of the transpose diffusive term for viscoplastic-type non-Newtonian fluid flows using a collocated variable arrangement, Numer. Heat Transfer Part B 67 (2015) 410–436.
[18] A. Walicka, J. Falicki, Reynolds number effects in the flow of an electro rheological fluid of Casson type between fixed surfaces of revolution, Appl. Math. Comput. 250 (2015) 639–649.
[19] I.L. Animasaun, E.A. Adebile, A.I. Fagbade, Casson fluid flow with variable thermo-physical property along exponentially stretching sheet with suction and exponentially decaying internal heat generation using the homotopy analysis method, J. Niger. Math. Soc. (2015) doi:10.1016/j.jnnms.2015.02.001 (in press).
[20] G. Sarojamma, K. Vendabai, Boundary layer flow of a Casson nanofluid past a vertical exponentially stretching cylinder in the presence of a transverse magnetic field with internal heat generation/absorption, Int. J. Mech. Aerosp. Ind. Mechatr. Eng. 9 (1) (2015).
[21] Y. Immanuel, P. Bapuji, C.K. Kirubhashankar, Casson flow of MHD fluid moving steadily with constant velocity, Appl. Math. Sci. 9 (30) (2015) 1503–1508.
[22] S. Ganesh, C.K. Kirubhashankar, A. Mohamed Ismail, Non-linear squeezing flow of Casson fluid between parallel plates, Int. J. Math. Anal. 9 (5) (2015) 217–223.
[23] M. Wahiduzzaman, M. Tajul Islam, P. Sultana, M. Afikuzzaman, MHD Couette flow of a Casson fluid between parallel porous plates, Prog. Nonlinear Dynamics Chaos 2 (2) (2014) 51–60.
[24] M. Wahiduzzaman, M. Musa Miah, M. Babul Hossain, F. Johora, S. Mistri, MHD Casson fluid flow past a non-isothermal porous linearly stretching sheet, Prog. Nonlinear Dynamics Chaos 2 (2) (2014) 61–69.
[25] S.K. Singh, B.S. Dandapat, Thin film flow of Casson liquid over a nonlinear stretching sheet in presence of uniform transverse magnetic field, Can. J. Phys. (2014) doi:10.1139/cjp-2014-0294.
[26] D.A.S. Rees, A.P. Bassom, Unsteady thermal boundary layer flows of a Bingham fluid in a porous medium, Int. J. Heat Mass transfer 82 (2015) 460–467.
[27] N. Sandeep, V. Sugunamma, Effect of inclined magnetic field on unsteady free convection flow of a dusty viscous fluid between two infinite flat plates filled by porous medium, J. Appl. Maths. Modell. 1 (2013) 16–33.
[28] N. Sandeep, V. Sugunamma, P. Mohan Krishna, Effects of radiation on an unsteady natural convective flow of a EG-Nimonic 80a nanofluid past an infinite vertical plate, Adv. Phys. Theor. Appl. 23 (2013) 36–43.
[29] P. Mohan Krishna, V. Sugunamma, N. Sandeep, Radiation and magneticfield effects on unsteady natural convection flow of a nanofluid past an infinite vertical plate with heat source, Chem. Process Eng. Res. 25 (2014) 39–52.
[30] C.S.K. Raju, M. Jayachandra Babu, N. Sandeep, V. Sugunamma, J.V. Ramana Reddy, Radiation and soret effects of MHD nanofluid flow over a moving vertical plate in porous medium, Chem. Process Eng. Res. 30 (2015) 9–23.
[31] A. Ishak, MHD boundary layer flow due to an exponentially stretching sheet with radiation effect, Sains Malays. 40 (2011) 391–395.
[32] S. Nadeem, S. Saleem, Analytical study of third grade fluid over a rotating vertical cone in the presence of nano particles, Int. J. Heat and Mass Transfer 85 (2015) 1041–1048.
[33] S. Nadeem, R. Mehmood, S.S. Motsa, Numerical investigations on MHD oblique flow of Walter's B type fluid over a convective surface, Int. J. Thermal Sci. 92 (2015) 162–172.
[34] S. Nadeem, S. Saleem, An optimized study of mixed convection flow of a rotating Jeffrey nanofluid on a rotating vertical cone, J. Comput. Theor. Nanosci. 12 (2015) 1–8.
[35] S. Nadeem, R. Mehmood, N.S. Akbar, Combined effects of magnetic field and partial slip on obliquely striking rheological fluid over a stretching surface, J. Magnet. Magn. Mater. 378 (2015) 457–462.
[36] M.Q. Brewster, Thermal Radiative Transfer Properties, John Wiley and Sons, New York, 1972.

Please cite this article in press as: C.S.K. Raju, N. Sandeep, V. Sugunamma, M. Jayachandra Babu, J.V. Ramana Reddy, Heat and mass transfer in magnetohydrodynamic Casson fluid over an exponentially permeable stretching surface, Engineering Science and Technology, an International Journal (2015), doi: 10.1016/j.jestch.2015.05.010